RAA 2015 Vol. **15** No. **1**, 37–44 doi: 10.1088/1674–4527/15/1/004
http://www.raa-journal.org *http://www.iop.org/journals/raa*

Research in Astronomy and Astrophysics

Structure function analysis of RISS and model-fitting to J1128+5925 *

Bin Liu, Bo Peng and Li-Jia Liu

National Astronomical Observatories, Chinese Academy of Sciences, Beijing 100012, China; *bliu@nao.cas.cn*

Received 2014 February 15; accepted 2014 May 15

Abstract There has been great progress recently in the study of radio variability, including the phenomenon of intraday variability (IDV) which occurs on short timescales of 50 h or less. There are two common explanations for IDV: an intrinsic mechanism or the effect of radio propagation through the interstellar medium. We consider the case of refractive interstellar scintillation (RISS), an extrinsic cause of radio variability. We theoretically derive the structure function of the 'thick screen' RISS model by using an approximation method, and discuss its application to the IDV phenomenon with some simulated results. Finally, the IDV source J1128+5925 is fitted with the 'thin screen' RISS model. Some possible combinations of parameters, namely source size, distance and relative velocity of the scattering screen, are presented.

Key words: radio variable source — refractive scintillation — structure function, IDV

1 INTRODUCTION

In extragalactic radio astronomy, radio sources with their flux varying on a short timescale of 50 h or less are called sources with intraday variability (IDV) (Witzel et al. 1986; Heeschen et al. 1987). The study of IDV is an important subject, since understanding the phenomenon of IDV deals with the problem of very high brightness temperature, introduces challenges to the emission mechanism and/or geometry of compact jet components, and provides a method to probe the interstellar medium (ISM). There are two common explanations for IDV, the intrinsic mechanism and the effect of radio propagation through the ISM (Wagner & Witzel 1995). Based on multi-wavelength observations, optical-radio correlations were found from the IDV source S5 0716+714 (Quirrenbach et al. 1991). For this source, it is possible that an intrinsic mechanism is dominant (Roland et al. 2009). However, there are still arguments against the radio-optical correlation (Bignall et al. 2003) and no more evidence has been reported. The detection of an annual cycle in the variability timescales of some sources that show extreme IDV, such as PKS 1257-326 (Bignall et al. 2003) and J1819+384 (Dennett-Thorpe & de Bruyn 2003), revealed the extrinsic nature of the sources due to their variability. Delays in the pattern arrival time between widely separated telescopes for sources with the fastest IDV give strong support to the extrinsic mechanism. In addition, the large MASIV VLA

* Supported by the National Natural Science Foundation of China.

Survey (Lovell et al. 2008) showed a correlation between IDV and the Hα emission measure, revealing a strong connection between IDV and the ionized ISM.

The emission regions of IDV sources are known to be very compact. Interstellar scintillation (ISS) will happen when radio waves from compact sources travel through the ISM (Rickett 1990). ISS can be divided into weak scintillation and strong scintillation, which includes refractive and diffractive ISS. Walker (1998) gives the frequency dependence for weak and strong ISS. The transition frequency varies from $\sim$ 8 to 40 GHz with Galactic latitude (see fig. 1 in Walker 1998). The values are approximate since the scattering is highly variable along a particular line of sight. In weak ISS, the ISM introduces small phase changes (< 1 rad) across the first Fresnel zone, while in strong ISS the wavefront is highly corrugated on scales smaller than the first Fresnel zone (Walker 1998). IDV studies at frequencies above a few GHz have been considered to be weak ISS due to the ISM within tens of parsecs from the Sun (Kedziora-Chudczer et al. 1997; Dennett-Thorpe & de Bruyn 2000; Rickett et al. 2002; Bignall et al. 2003, 2006; Gabányi et al. 2007). The appearance of IDV is more common towards nearby scattering material, as the timescale of ISS produced in more nearby "screens" is shorter, and also the limiting angular size for a source to scintillate is larger, compared with more distant scattering material.

As discussed by Rickett et al. (1984), refractive interstellar scintillation (RISS) introduces slow, broadband variations at low frequencies. The contribution of RISS to the flux variability depends on the observing frequency and the properties of the scattering along the line of sight. In this paper, we discuss RISS as a possible extrinsic explanation for IDVs. The discussion is limited to the case of strong scintillation and frequencies around or lower than the transition frequency.

In the RISS model of Narayan (1992), the ISM is treated as a scattering screen which is perpendicular to the direction of radio propagation. There are density fluctuations in the interstellar plasma which cause the medium to act as a "concave lens" or "convex lens." The radiation can be either focused or defocused by the medium. As a consequence of the relative speed between the screen and the observer, the phenomenon of radio variability can be observed (see Fig. 1). The scattering angle induced by the RISS effect is proportional to $\delta N \lambda^2$, where δN is the fluctuation of the electron density in the ISM and λ is the observed wavelength of radiation from a radio source (Romani et al. 1986). For one dimensional refraction, the amplitude of the focusing and defocusing is proportional to $\delta N \lambda^2 / \theta$, where θ is the angular size of the radio source. The RISS occurs when $L\theta \ll \lambda_N$. λ_N is the scale of fluctuations in the electron density and L is the distance between the screen and the observer. Because of motion in the ISM with respect to Earth, the scintillation pattern sweeps across the Earth. The flux of a radio source varies with the concentration and diffusion of radiation. The characteristic timescale is $L\theta / v\sqrt{2}$, where v is the sweep speed.

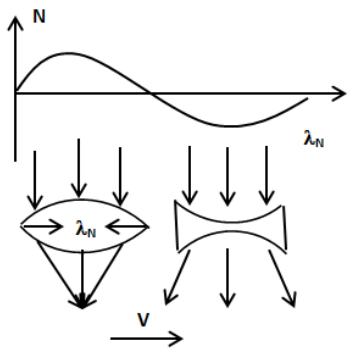

Fig. 1 Schematic diagram of RISS.

In Section 2, the structure function of the 'thick screen' RISS model is derived by using a new approximation method and its application to the IDV phenomenon with some simulated results is discussed. Section 3 gives the result of the fitting to the IDV source J1128+5925 with the 'thin screen' RISS model. Some possible combinations of parameters, namely source size, distance and relative velocity of the scattering screen, are presented. Conclusions are provided in Section 4.

2 STRUCTURE FUNCTION OF RISS

To study variable sources, the structure function of flux density variations is used to calculate the characteristic timescale (Simonetti et al. 1985). Based on the RISS model developed by Romani et al. (1986) and Cordes et al. (1984), Qian et al. (1995) calculate the structure function of intensity fluctuations produced by the scattering medium. Following the work of Qian et al. (1995), a simplified RISS model is presented with a new approximation method, which is applied to simplify the derivation of the structure function for the case of RISS in an extended medium.

2.1 Derivation of the Formula

Using the flux autocorrelation function to express the structure function, the relation was given by Qian et al. (1995)

$$F(\tau) \;=\; \langle \delta F(t) \delta F(t+\tau) \rangle_t \,, \tag{1}$$

$$D(\tau) \;=\; F(0) - F(\tau) \,, \tag{2}$$

where F is the autocorrelation function, τ is the time lag, $\langle \cdots \rangle_t$ means averaging over the period t and D is the structure function. According to the theory of RISS developed by Romani et al. (1986), the flux autocorrelation function of RISS has a Gaussian form. With the relation described in Section 1, $F(\tau)$ can be expressed as

$$F(\tau) = \frac{\overline{N^2}\lambda^4}{\theta^2} \exp\Big(-\frac{\tau^2}{\tau_0^2}\Big) \,, \tag{3}$$

where $\tau_0 = L\theta/(\frac{v}{\sqrt{2}})$. For simplicity, we use N instead of δN to stand for the electron density fluctuation. The overline represents the average value of the squares of density fluctuations due to multiple plasmas with different λ_N. Armstrong et al. (1995) have shown that the electron density power spectrum of the ISM can be described by a power-law model.

$$\overline{N^2} = N_0^2 k^{-\beta}, \tag{4}$$

where N_0^2 is a constant with the unit of spectral density, $k = \frac{2\pi}{\lambda_N}$ and for a Kolmogorov spectrum $\beta = 11/3$. Sometimes $\beta = 4$ is chosen for simplicity. Equations (1), (2) and (3) can be used to describe the simplified thin screen model of RISS. When τ is small,

$$D(\tau) \propto \tau^2. \tag{5}$$

From observations given by Simonetti et al. (1985), some radio sources follow this rule, while some others have a different relation

$$D(\tau) \propto \tau^p, \tag{6}$$

where $1 < p < 2$.

In the latter case, a thin screen model cannot be applied and a model with a continuous medium should be considered (Blandford & Narayan 1985). Assuming that the density distribution for scattering in the medium has a Gaussian form (Qian et al. 1995 and Cordes et al. 1984),

$$\frac{d\overline{N^2(L)}}{dL} = \frac{2N_0^2}{\sqrt{\pi}H} \exp\Big(-\frac{L^2}{H^2}\Big), \tag{7}$$

where H is the thickness of the screen. Taking $y = \frac{L}{H}$ and combining Equation (3) and Equation (7), we obtain

$$F(\tau) = \frac{2N_0^2\lambda^4}{\sqrt{\pi}\theta^2}\int_0^\infty \exp(-y^2)\exp\Big(-\frac{v^2\tau^2}{2H^2\theta^2y^2}\Big)dy\,, \tag{8}$$

where θ is its first-order approximation (see Qian et al. 1995). Equation (8) is the flux autocorrelation function of a thick-screen model, which does not depend on the power-law spectral index of electron density.

Here an approximation method is taken to simplify Equation (8). For the integral part, an approximate relation is applied,

$$\int_0^\infty \exp(-t^2)\exp\Big(-\frac{a^2}{t^2}\Big)dt \approx \int_a^\infty \exp(-t^2)dt\ (a \ll 1)\,. \tag{9}$$

From the properties of the error function,

$$\mathrm{erf}\,(y_0) = \frac{2}{\sqrt{\pi}}\int_0^{y_0}\exp(-t^2)dt, \tag{10}$$

$$\mathrm{erfc}\,(y_0) = 1 - \mathrm{erf}\,(y_0) = \frac{2}{\sqrt{\pi}}\int_{y^0}^\infty \exp(-t^2)dt\ (a \ll 1). \tag{11}$$

Using Equations (9)[1], (10) and (11), we have

$$F(\tau) \approx \frac{N_0^2\lambda^4}{3\theta^2}\mathrm{erfc}\,(y_0), \tag{12}$$

where

$$y_0 = \frac{(v/\sqrt{2})\tau}{H\theta}. \tag{13}$$

The structure function is obtained by substituting Equation (12) into Equation (2)

$$D(\tau) \approx \frac{N_0^2\lambda^4}{3\theta^2}\mathrm{erf}\,(y_0)\,. \tag{14}$$

When $y_0 = 1$, the saturated timescale is

$$\tau_{\mathrm{sat}} = \frac{H\theta}{v/\sqrt{2}}\,. \tag{15}$$

As an approximation of the error function

$$\mathrm{erf}\,(x) = \frac{2}{\sqrt{\pi}}\sum_{n=0}^{\infty}\frac{(-1)^n x^{2n+1}}{(2n+1)n!} = \frac{2}{\sqrt{\pi}}(x - \frac{x^3}{3} + \frac{x^5}{10} - \frac{x^7}{42} + \frac{x^9}{216} - \cdots)\,. \tag{16}$$

When τ is small, $y_0 \ll 1$. Substituting Equation (16) into Equation (14), the structure function is derived as

$$D(\tau) \approx \sqrt{\frac{2}{\pi}}\frac{N_0^2\lambda^4}{3H\theta^3}v\tau\Big(1 - \frac{v^2\tau^2}{6H^2\theta^2}\Big)\,. \tag{17}$$

The structure function given by Equation (15) is the simplified form of Equation (14). When $\tau \leq \tau_{\mathrm{sat}}$, then $y_0 \leq 1$ and Equation (14) is valid. Therefore, Equation (15) has the limitation $\tau < \tau_{\mathrm{sat}}$. However, it is easier to obtain the variability timescale with Equation (15). Note that the timescales referred to are characteristic timescales since RISS is a stochastic process and does not produce periodic variations.

[1] Equation (9) is confirmed by numerous simulations.

2.2 Numerical calculation

Equation (17) is the structure function of a thick-screen RISS model, in which $D(\tau)$ depends on λ, θ, H and v. Expressing λ in cm, θ in mas, H in kpc and v in km s^{-1}, Equation (13) can be rewritten as

$$y_0 = 4.08 \times 10^{-4} \frac{v\tau}{H\theta}. \tag{18}$$

The next step is to perform some numerical calculations to find reasonable timescales. The angular size θ is given by Qian et al. (1995)

$$\theta^2 = \theta_i^2 + \theta_s^2, \tag{19}$$

$$\begin{cases} \theta_i \approx 3.6\lambda(\mathrm{mas}) \\ \theta_s \approx 4\lambda(1+0.7\lambda^2)^{\frac{1}{2}} \end{cases}, \tag{20}$$

where θ_i is the intrinsic angle and θ_s is the scattering angle. Equation (20) is obtained by Cordes et al. (1984) under assumptions for a source flux density of 1 Jy and brightness temperature of 5×10^{11} K, using the expected scattering strength from Cordes et al. (1984) for a Galactic latitude of 30°. Following the relationship given by Romani et al. (1986), we have

$$N_0^2 = 1.6 \times 10^{-21} H\,. \tag{21}$$

Substituting Equations (18) and (21) into Equation (17), the timescale is obtained by setting the derivative of $D(\tau)$ to zero. Assuming that 40% of the half thickness of the Galactic disk (1 kpc) contributes, the value of the thickness of the screen $H = 0.4$ kpc. The typical sweep speed is assumed to be $v = \sqrt{\frac{2}{3}} \times 30$ km s^{-1} if it is mainly contributed by Earth's orbital speed. The results are given in Table 1 at values of the wavelength λ of $3.6, 6, 11$ and 20 cm.

The timescales listed in Table 1 are several weeks, much longer than that of IDV. In the RISS model of extragalactic radio sources, the parameters v and H can be modified to fit IDV timescales. Considering the case with a lower scatter broadening than assumed in Equation (20) and that extragalactic sources contain a fraction of their flux density in a very compact and high brightness temperature component, a smaller angular size could be taken to reach a shorter timescale. Qian (1994) tried to decrease the angular size by one order of magnitude. Taking $\theta \approx 0.36\lambda$ (Qian 1994), $H = 0.25$ kpc and $v = \sqrt{\frac{2}{3}} \times 30$ km s^{-1}, the results are shown in Figures 2–5. In Figures 2–5, the slopes of the linear parts are equal to 1. As is mentioned in Section 2.1, the approximation of the structure function is valid for $0 \leq \tau \leq \tau_{\mathrm{sat}}$. In the figures, τ_{sat} is the maximum value.

Table 2 lists the timescales at different wavelengths. The timescales are at the same level as those observed in IDV sources. The parameters v, H and θ cannot be uniquely derived by only a single observation. Observation of an annual cycle would help to constrain the parameters.

Table 1 The Result of the RISS Simulation (1)

λ (cm) (1)	θ (mas) (2)	τ (d) (3)
20	1.08	43.4
11	0.59	23.7
6	0.32	12.9
3.6	0.19	7.7

Notes: Column (1) is the wavelength, Col. (2) the angle and Col. (3) the timescale.

Table 2 The Result of the RISS Simulation (2)

λ (cm) (1)	θ (mas) (2)	τ (d) (3)
20	0.072	1.8
11	0.04	0.99
6	0.022	0.54
3.6	0.013	0.32

Notes: same as Table 1.

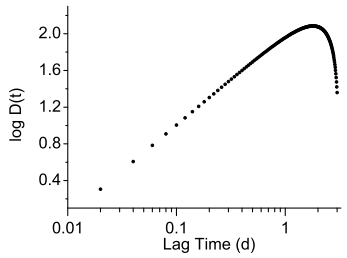

Fig. 2 Structure function at 20 cm on a timescale of $\tau = 1.8$ d.

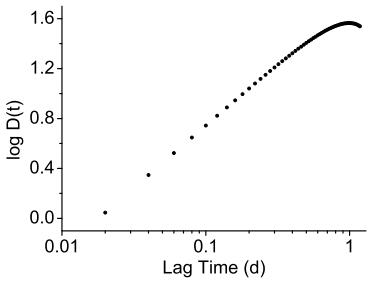

Fig. 3 Structure function at 11 cm on a timescale of $\tau = 0.99$ d.

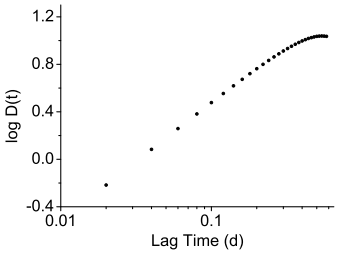

Fig. 4 Structure function at 6 cm on a timescale of $\tau = 0.54$ d.

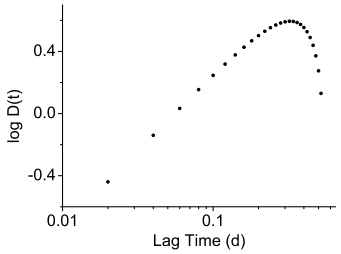

Fig. 5 Structure function at 3.6 cm on a timescale of $\tau = 0.32$ d.

3 RISS FITTING TO THE IDV SOURCE J1128+5925

Annual modulation is strong evidence for extrinsic variability in the source, which may indicate RISS. Because of the orbital motion of the Earth, the relative speed between the observer and the screen changes during a year. Consequently, the timescales of IDV change annually. The radio source J1128+5925 shows IDV with an annual modulation (Gabányi et al. 2007). The basic idea of this work is to see if the RISS model can provide reasonable parameters for this source. If so, this RISS model fitting can provide useful information on the ISM.

Gabányi et al. (2007) plotted the structure function calculated from observational data. According to the slope of the structure function ($p \approx 2$), they concluded that the thin screen model should be applied for this case. From Equation (2),

$$F(\tau) = \frac{\overline{N^2}\lambda^4}{\theta^2} \exp\Big(-\frac{v^2\tau^2}{2\theta^2 L^2}\Big). \tag{22}$$

Taking the scattering strength Q_0 instead of the electron density fluctuation N, we use (Qian et al. 1995)

$$F(\tau) = \frac{Q_0\lambda^4}{(2\pi)^5\theta^2} \exp\Big(-\frac{v^2\tau^2}{2\theta^2 L^2}\Big), \tag{23}$$

where $Q_0 = 1.6 \times 10^{21} C_{-4} L$. Substituting Equation (23) into Equation (2), the structure function is

$$D(\tau) = \frac{Q_0\lambda^4}{(2\pi)^5\theta^2} \left[1 - \exp\Big(-\frac{v^2\tau^2}{2\theta^2 L^2}\Big)\right]. \tag{24}$$

Taking $D(\tau)' = 0$, the timescale is obtained as,

$$\tau_0 = L\theta/\Big(\frac{v}{\sqrt{2}}\Big)\,. \tag{25}$$

Gabányi et al. (2007) have presented the timescales for this source, which were calculated from the observational data by a structure function. Two data sets observed at 4.85 GHz on 2005 September 16 and 2006 April 28 are chosen for the model fitting. The timescales are 0.5 ± 0.1 and 1.4 ± 0.1 d, which are at nearly the two extremes in an annual cycle. The time lag between the two observations is about six months. The timescale varies mainly because the relative speed between observer and the screen changes, depending on the direction of the Earth's motion.

Equation (25) is used to calculate the parameter v. The parameters θ and L are fixed at first. Then the two timescales are calculated by varying the value of v. Because the parameters θ, L and v are combined ($\theta L/v$) in Equation (25), a single v may give several pairs of θ and L. We let θ range from 0.05 to 0.5 mas, and L varies from 0.05 to 1 kpc. Considering the projection of the Earth's speed and the typical velocity of ionized gas in the Galaxy, the range of v is set from 10 to 100 km s^{-1}. Because the projection of the Earth's speed, which contributes to the sweep speed, is less than 30 km s^{-1} and the speed of the screen is expected to be of the same order, the fitted values for speed pairs (36.8, 13.1) and (49.0, 17.5) are reasonable. Then we have the value of speed fixed and vary the values of the (θ, L) pair to produce the 1σ uncertainty of τ. The errors of θ and L are given as the maximum deviations.

The preferred results are given in Table 3.

Table 3 The RISS Model Fitting Result

θ (mas) (1)	L (kpc) (2)	$v(\tau = 0.5 \pm 0.1\mathrm{d})$ (km s^{-1}) (3)	$v(\tau = 1.4 \pm 0.1\mathrm{d})$(km s^{-1}) (4)
0.05 ± 0.01	0.15 ± 0.03	36.8	13.1
0.15 ± 0.03	0.05 ± 0.01		
0.05 ± 0.01	0.2 ± 0.04		
0.1 ± 0.02	0.1 ± 0.02	49.0	17.5
0.2 ± 0.04	0.05 ± 0.01		

Notes: Columns (1) and (2) give the angular size of the source and the screen distance; Columns (3) and (4) the sweep speeds corresponding to the two timescales of 0.5 and 1.4 d respectively.

However, the speed listed above is a transverse component. To get the velocity of the ISM with respect to the local standard of rest, a projection angle has to be considered when more observational data are available. For the source J1128+5925, if L is larger than 100 pc, its angular size should be less than 100 μas; on the other hand, if its angular size is bigger than 0.2 mas, the screen distance L must be less than 50 pc. In addition, the RISS model fitting is to the data observed at 4.85 GHz, which according to the Galactic latitude of this source and the frequency dependence relation given by Walker (1998) is below the transition frequency of ∼8 GHz. The frequency dependence needs to be further examined with observations at other frequencies.

4 CONCLUSIONS

In this paper, the structure function of RISS has been theoretically derived with an approximation method, and has been applied to the phenomenon of IDV.

The idea to derive a structure function for the RISS model is the same as the traditional method (Blandford & Narayan 1985), but the description of some physical details is different, and an approximation for the error function was used in our method. This simplified the derivation.

In our study, timescales of several weeks are produced by a numerical simulation of the structure function, in which traditional values of parameters are adopted. To reach the IDV timescale, a smaller

angular size and thinner thickness of screen are applied. This work shows the possibility using the RISS model to explain the phenomenon of IDV. However, the parameters should be further explored by more observations and discussion. Most pulsars lie near the Galactic plane. For extragalactic sources at high Galactic latitude, the value of H may be smaller. Smaller H yields a smaller value of timescale. In addition, the fact that the nearby scattering material dominates the ISS of active galactic nuclei will affect the value of H.

As an example J1128+5925, which is an IDV source with annual modulation, is fitted by the RISS model. With the timescales of this source, we obtained some reasonable values for θ, L and v. There are several IDV sources found with annual modulation, for example J1819+3845 (Dennett-Thorpe & de Bruyn 2003) and PKS 1257-326 (Bignall et al. 2006), in which the scintillation models were applied successfully.

Acknowledgements The authors thank Prof. Wenjun Han for the helpful discussion. We appreciate the anonymous referee, who gave many careful comments that improved our work in this paper. This work was supported by the National Basic Research Program of China (973 program, Grant No. 2013CB837900) and the National Natural Science Foundation of China (Grant No. 11303057).

References

Armstrong, J. W., Rickett, B. J., & Spangler, S. R. 1995, ApJ, 443, 209
Bignall, H. E., Jauncey, D. L., Lovell, J. E. J., et al. 2003, ApJ, 585, 653
Bignall, H. E., Macquart, J.-P., Jauncey, D. L., et al. 2006, ApJ, 652, 1050
Blandford, R., & Narayan, R. 1985, MNRAS, 213, 591
Blandford, R., Narayan, R., & Romani, R. W. 1986, ApJ, 301, L53
Cordes, J. M., Ananthakrishnan, S., & Dennison, B. 1984, Nature, 309, 689
Dennett-Thorpe, J., & de Bruyn, A. G. 2000, ApJ, 529, L65
Dennett-Thorpe, J., & de Bruyn, A. G. 2003, A&A, 404, 113
Gabányi, K. É., Marchili, N., Krichbaum, T. P., et al. 2007, A&A, 470, 83
Heeschen, D. S., Krichbaum, T., Schalinski, C. J., & Witzel, A. 1987, AJ, 94, 1493
Kedziora-Chudczer, L., Jauncey, D. L., Wieringa, M. H., et al. 1997, ApJ, 490, L9
Lovell, J. E. J., Rickett, B. J., Macquart, J.-P., et al. 2008, ApJ, 689, 108
Narayan, R. 1992, Royal Society of London Philosophical Transactions Series A, 341, 151
Qian, S. J. 1994, Acta Astrophysica Sinica, 14, 333
Qian, S. J., Britzen, S., Witzel, A., et al. 1995, A&A, 295, 47
Quirrenbach, A., Witzel, A., Wagner, S., et al. 1991, ApJ, 372, L71
Rickett, B. J. 1990, ARA&A, 28, 561
Rickett, B. J., Coles, W. A., & Bourgois, G. 1984, A&A, 134, 390
Rickett, B. J., Kedziora-Chudczer, L., & Jauncey, D. L. 2002, ApJ, 581, 103
Roland, J., Britzen, S., Witzel, A., & Zensus, J. A. 2009, A&A, 496, 645
Romani, R. W., Narayan, R., & Blandford, R. 1986, MNRAS, 220, 19
Simonetti, J. H., Cordes, J. M., & Heeschen, D. S. 1985, ApJ, 296, 46
Wagner, S. J., & Witzel, A. 1995, ARA&A, 33, 163
Walker, M. A. 1998, MNRAS, 294, 307 (Erratum: Walker, M. A., 2001, MNRAS, 321, 176)
Witzel, A., Heeschen, D. S., Schalinski, C., & Krichbaum, T. 1986, Mitteilungen der Astronomischen Gesellschaft Hamburg, 65, 239